PERGAMON

International Journal of Solids and Structures 36 (1999) 4789–4804

INTERNATIONAL JOURNAL OF SOLIDS and STRUCTURES

On the coupling of 3D BEM and FEM frame model applied to elastodynamic analysis

H.B. Coda*, W.S. Venturini

São Carlos School of Engineering, University of São Paulo, Av. Carlos Botelho 1465, 1356-970 São Carlos, Brazil

Received 5 May 1998; accepted 8 September 1998

Abstract

This work presents the coupling of framed structures approached by finite elements with three-dimensional bodies represented by the boundary element method. The coupling is particularly dedicated to analyse three-dimensional half space stiffened by piles and other composite domain problems, for which static and dynamic cases have been taken into account. Some numerical examples are analysed to point out the power and the accuracy of the proposed scheme.

Keywords: Transient elastodynamic analysis; Boundary elements; Finite elements; Coupling; Soil structure interaction

1. Introduction

Over the last few years a lot of progress has been made in boundary/finite element coupling techniques. This procedure is particularly recommended to analyse soil-structure interactions, where the advantages of each method can be taken. The main developments regarding BEM/FEM combinations are not discussed in this article, but comprehensive reviews can be found, for instance, in Stamos and Beskos (1995) and Beer and Watson (1992). The progress of the boundary element method for numerical solutions for elastodynamic problems is completely reported in two important reviews made by Beskos (1987, 1997) in which the major developments in that area until 1997 are resumed. For this work, it is also convenient to point out three recent publications: Luco and Barros (1994), where a 3D BEM/FEM coupling dedicated to frequency domain problems is presented; Antes and Steinfield (1992), dealing with 3D BEM/BEM coupling in time domain; and Guan and Novak (1994), to analyse 2D transient problems using a BEM formulation combined with rigid strips. The authors have given some contribution to this subject, particularly related to 3D time domain BEM/FEM and BEM/BEM couplings applied to the following interaction cases: plate/soil (Barreto et al., 1996), shell/soil (Coda and Venturini., 1996d), rigid foot/soil (Coda and Venturini, 1995a) and massive block/soil (Coda and Venturini, 1995b).

* Corresponding author. E-mail: hbcoda@sc.usp.br

0020-7683/99/$ - see front matter
PII: S0020-7683(98)00265-0

In the present work, the authors intend to show a simple procedure to connect beam finite elements with a three-dimensional medium described by either static or dynamic BEM algebraic representations. For the dynamic case, only the time domain approach will be considered. By using this kind of coupling, some important practical cases, buildings/soil interaction, buried steel bars in a concrete body and other composed domains can now be accurately analysed.

The work presentation is organised into three sections. In the first section, BEM elastostatic and elastodynamic formulations are presented, including a discussion on the cylindrical element adopted to describe the interface between beams and the 3D domain. Then, the classical finite element approach for framed structures, considering both the static and dynamic cases, are adapted to make easy to achieve the BEM/FEM coupled model, based on the consistent lumping matrix. The matrix arrangement followed for this coupling makes possible to specify as unknowns the contact forces between the beam boundary and the surface of the cylindrical hole present inside the 3D medium. In the third section, the FEM/BEM coupled algebraic system of equations is achieved by using the sub-region technique, completed by some recommendations on the step by step data manipulation.

Having presented the bases of the proposed BEM/FEM coupling technique, three examples are taken to illustrate its applicability, accuracy and advantages.

2. Boundary element formulation

The BEM formulations for the elastostatic and elastodynamic problems are based on Somigliana and Graffis' reciprocal theorems, respectively.

For elastostatic domain Ω with boundary Γ, one has:

$$C_{ki}(S)u_i(S) = \int_\Gamma u^*_{ki}(S,Q)p_i(Q)\,\mathrm{d}\Gamma(Q) - \int_\Gamma u_i(Q)\,p^*_i(S,Q)\,\mathrm{d}\Gamma(Q) + \int_\Omega b_i(q)u^*_{ki}(S,q)\,\mathrm{d}\Omega(q) \tag{1}$$

in which b_i is the body force field and q and s (or Q and S when defied along Γ) represent field and load points, respectively. The star superscript denotes Kelvin's fundamental solution and C_{ik} is the classical free term.

In order to transform the above integral representation into an algebraic one, quadratic isoparametric boundary elements with eight nodes have been adopted to approach boundary values, while quadratic isoparametric cells with twenty nodes were taken to approximate domain values. It is important to describe a particular boundary element adopted in this formulation to approach cylindrical surfaces. That element is employed to describe the interface surface between beams and the 3D elastic medium and also to approximate the interactive force field over that contact area.

Two nodes and the beam radius, as illustrated in Fig. 1, define the cylindrical element. The element geometry and the tractions acting over the surface are assumed to be linear in the longitudinal direction and constant in the θ angular co-ordinate direction. By assuming this approximation, only two shape functions are required to describe the geometry and to approach the traction values over the element, as follows,

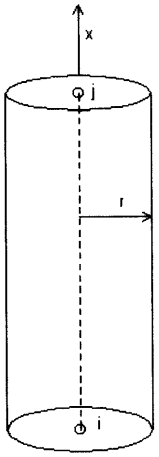

Fig. 1. Cylindrical boundary element.

$$P_i = \phi_1 P_i^1 + \phi_2 P_i^2 \tag{2a}$$

$$u_i = \phi_1 U_i^1 + \phi_2 U_i^2 \tag{2b}$$

$$x_i = \phi_1 X_i^1 + \phi_2 X_i^2 + R n_i(\theta) \tag{2c}$$

where ϕ_k represents the linear interpolation function, X_i^α is the local Cartesian co-ordinate, α gives the element nodes, R is the beam radius and $n_i(\theta)$ is the unit normal vector component referred to the cylindrical surface.

It is worth stressing that only surface forces have been approximated over the cylindrical surface in the same sense described by Ferro and Venturini (1992) for the static case. The interface nodes are internal points defined along the beam axis, while the interface forces are computed at nodes defined over the actual beam surface; i.e. the integral and corresponding algebraic representations are written for collocations defined along the beam axis, while field points are taken over the interface. Displacements could be approximated as shown in expression (2), but it does not improve the final results; instead it increases the amount of computing.

In order to perform numerically the integrals over boundary elements, sub-elements are adopted following a well-known technique very often employed to solve transient problems based on elastodynamic BEM formulations (Lachat and Watson, 1976). In this technique, fine mesh refinement is required when the collocation point is near the integrated element. The sub-element mesh can be coarser when the distance between the load point and the element, or sub-element, increases. The singular integrals, found when the collocations are defined over the element, are performed by means of a numerical procedure based on Kutt's quadrature formula (Kutt, 1975; Coda and Venturini, 1995c).

Taking into account the described approximations, the following classical BEM system of algebraic equations is achieved,

$$H\mathbf{U} = G\mathbf{P} + \mathbf{B} \tag{3}$$

Solving eqn (3) one finds all unknown boundary values, and the internal values are computed appropriately (Brebbia et al., 1984; Brebbia and Domingues, 1984).

Similarly, for elastodynamic one can adopt the Graffis' reciprocal theorem to find:

$$C_{ki}(Q,s)\int_0^t u_i(s,\tau)f(t-\tau)\,\mathrm{d}\tau = \int_0^t\int_\Gamma u^*_{ki}(Q,t-\tau;s/f)p_i(Q,\tau)\,\mathrm{d}\Gamma\,\mathrm{d}\tau + \int_0^t\int_\Gamma u_i(Q,\tau)p^*_{ki}(Q,t-\tau;s/f)\,\mathrm{d}\Gamma\,\mathrm{d}\tau + \int_0^t\int_\Omega u^*_{ki}(q,t-\tau;s/f)b_i(q,\tau)\,\mathrm{d}\Omega\,\mathrm{d}\tau \quad (4)$$

where u^*_{ki} and p^*_{ki} are fundamental values, or general Stokes' state (Mansur, 1988; Stokes, 1849; Karabalis and Beskos, 1984), obtained by choosing appropriately the impulse distribution $f(\tau)$ in eqn (4) and C_{ki} is an independent free term, similar to those obtained for elastostatic formulations.

Adopting the following unit impulse distribution along a time step Δt (Coda, 1993; Coda and Venturini, 1996a–c),

$$f(\tau) = [H(\tau)-H(\tau-\Delta t)]/\Delta t \quad (5)$$

in which $H(t)$ is the Heaviside function, eqn (4) becomes:

$$C_{ki}(Q,s)\int_{t-\Delta t}^t \frac{u_i(s,\tau)}{\Delta t}\,\mathrm{d}\tau = \int_0^t\int_\Gamma u^*_{ki}(Q,t;s,\tau)p_i(Q,\tau)\,\mathrm{d}\Gamma\,\mathrm{d}\tau - \int_0^t\int_\Gamma u_i(Q,\tau)p^*_{ki}(Q,t;s,\tau)\,\mathrm{d}\Gamma\,\mathrm{d}\tau + \int_0^t\int_\Omega u^*_{ki}(q,t;s,\tau)b_i(q,\tau)\,\mathrm{d}\Omega\,\mathrm{d}\tau \quad (6)$$

Although any time approximation function may be used together with the adopted fundamental solution (Heaviside load function), the constant approximation has been chosen due to its efficiency and accuracy observed in many numerical analyses carried out.

In eqn (6), the spatial integrals are performed by adopting the same boundary elements and internal cells described for the elastostatic case. Both singular and non-singular collocation approaches are considered (Coda and Venturini, 1995d). The singular integrals are carried out by a direct scheme based on the Kutt's quadrature formula (Kutt, 1975; Coda and Venturini, 1995c). The classical Gauss' integration scheme has been adopted to carry out the non-singular, together with the well-known element sub-division technique (Lachat and Watson, 1976).

After performing the described time and spatial element integrations one achieves the final set of algebraic equations for the elastodynamic problem:

$$H^\theta\mathbf{U}^\theta = G^\theta\mathbf{P}^\theta \quad (7)$$

in which $\theta = 1,\ldots,N_t$ and summation is implied in θ.

Due to its nature, the fundamental solution vanishes after some period of time, therefore the matrices are computed only for a limited number of time steps given by,

$$N_t = \frac{d_{\max}}{C_2\Delta t} + 1 \quad (8)$$

where $d_{\max}$ is defined as the maximum length inside the discretized solid.

3. Frame structure algebraic relations

In order to consider either the 3D medium reinforced by internal bars or connected to 3D frames, it is necessary to write beam FEM algebraic relations properly modified to assure good numerical answers using a simple and reliable scheme. The algebraic beam relations, for static or dynamic elastic analyses, can be derived from the general formulation of the finite element method (Zienkiewicz, 1980; Clough and Penzien, 1975; Bathe, 1982).

Having derived properly the FEM algebraic relations of a frame element considering mass and damping terms the following matrix equation can be easily written,

$$H\mathbf{U} + C\dot{\mathbf{U}} + M\ddot{\mathbf{U}} = G\mathbf{P} + \mathbf{F} \tag{9}$$

where the BEM notation has been adopted for convenience. Herein, mass, stiffness and damping matrices are denoted by M, H and C respectively; while $\dot{\mathbf{U}}$ and $\ddot{\mathbf{U}}$ are velocity and acceleration vectors and $\mathbf{F}$ represents the body and concentrated forces.

In order to make simple the coupling between BEM and FEM sets of algebraic equations, the interface or interactive equivalent nodal forces are kept into their expanded forms, given by the product $G\mathbf{P}$. In this sense, G is called the consistent lumping matrix.

The FEM formulation is taken in this work only to approach simple beam elements for which Bernoulli–Navier hypothesis is assumed to govern the strain distribution over the cross section. Cubic approximations are chosen to approach transversal displacements, while linear shape functions are adopted to approach longitudinal and torsional displacements. The distributed surface load is assumed linear in the longitudinal direction and constant along the circumferential direction as it has been made to define the BEM cylindrical element. Figure 2 shows the relevant nodal values taken to write the algebraic equations, three translations, three rotations, three forces and the twisting moments defined at each node.

The matrices H and M shown in eqn (9) are the standard ones easily found in the literature when the described approximations are adopted, while the distributed interactive forces give the following lumping matrix G,

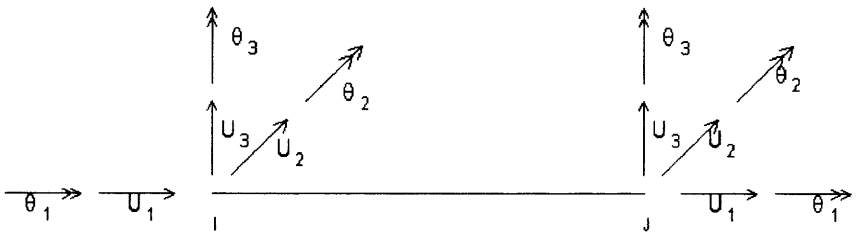

Fig. 2. Beam finite element; degrees of freedom.

$$G = 2\pi R$$

$$\begin{bmatrix}
L/3 & 0 & 0 & 0 & 0 & 0 & L/6 & 0 & 0 & 0 & 0 & 0 \\
0 & 7L/20 & 0 & 0 & 0 & 7L/20 & 0 & 3L/20 & 0 & 0 & 0 & 3L/20 \\
0 & 0 & 7L/20 & 0 & 7L/20 & 0 & 0 & 0 & 3L/20 & 0 & 3L/20 & 0 \\
0 & 0 & 0 & L/3 & 0 & 0 & 0 & 0 & 0 & L/6 & 0 & 0 \\
0 & 0 & -L^2/20 & 0 & -L^2/20 & 0 & 0 & 0 & -L^2/30 & 0 & -L^2/30 & 0 \\
0 & L^2/20 & 0 & 0 & 0 & L^2/20 & 0 & L^2/30 & 0 & 0 & 0 & L^2/30 \\
L/6 & 0 & 0 & 0 & 0 & 0 & L/3 & 0 & 0 & 0 & 0 & 0 \\
0 & 3L/20 & 0 & 0 & 0 & 3L/20 & 0 & 7L/20 & 0 & 0 & 0 & 7L/20 \\
0 & 0 & 3L/20 & 0 & 3L/20 & 0 & 0 & 0 & 7L/20 & 0 & 7L/20 & 0 \\
0 & 0 & 0 & L/6 & 0 & 0 & 0 & 0 & 0 & L/3 & 0 & 0 \\
0 & 0 & L^2/30 & 0 & L^2/30 & 0 & 0 & 0 & L^2/20 & 0 & L^2/20 & 0 \\
0 & -L^2/30 & 0 & 0 & 0 & -L^2/30 & 0 & 0 & -L^2/20 & 0 & 0 & -L^2/20
\end{bmatrix} \tag{10}$$

where L and R represent the following beam parameters: length and radius, respectively.

In order to integrate eqn (9) the adopted time step algorithm was the well-known Newmark β scheme, which is algebraically represented by (Warburton, 1976),

$$\left[M + \frac{1}{2}(\Delta t)C + \beta(\Delta t)^2 H\right]\mathbf{U}_{s+1} = (\Delta t)^2[\beta G\mathbf{P}_{s+1} + (1-2\beta)G\mathbf{P}_s + \beta G\mathbf{P}_{s-1}]$$
$$+ (\Delta t)^2[\beta(\mathbf{B}+\mathbf{F})_{s+1} + (1-2\beta)(\mathbf{B}+\mathbf{F})_s + \beta(\mathbf{B}+\mathbf{F})_{s-1}]$$
$$+ [2M - (\Delta t)^2(1-2\beta)H]\mathbf{U}_s - \left[M - \frac{1}{2}(\Delta t)C + \beta(\Delta t)^2 H\right]\mathbf{U}_{s-1} \tag{11}$$

After considering either the above integration scheme or any other alternative procedure, eqn (9) can be properly rearranged to be represented by the same form adopted to express the BEM relations, as follows:

$$H\mathbf{U} = G\mathbf{P} + \mathbf{A} \tag{12}$$

where $\mathbf{A}$ is an independent vector and $\mathbf{U}$ and $\mathbf{P}$ are the actual problem variables.

4. BEM/FEM coupling

In order to couple BEM with FEM formulations, the classical sub-region technique has been adopted here. This procedure is very general, allowing combinations of many sub-domains discretized by either FEM or BEM. As the final matrices contain blocks of zeros and can be partially symmetric, several solution schemes may be adopted to achieve the unknown values of $\mathbf{U}$ and $\mathbf{P}$ (Stamos and Beskos, 1995).

Taking two sub-regions Ω_i and Ω_j, with a common interface Γ_{ij}, one can write eqn (12) for each one to find,

$$H^i\mathbf{U}^i = G^i\mathbf{P}^i + \mathbf{A}^i \tag{13a}$$

$$H^j\mathbf{U}^j = G^j\mathbf{P}^j + \mathbf{A}^j \tag{13b}$$

Taking into account only the values along the interface Γ_{ij}, the equilibrium and geometrical compatibility conditions are represented by,

$$\mathbf{U}^{ij} = \mathbf{U}^{ji} \quad \text{and} \quad \mathbf{P}^{ij} = -\mathbf{P}^{ji} \tag{14a,b}$$

where the superscripts indicate the sub-regions belonging to the interface.

The vectors $\mathbf{U}^{ij}$ and $\mathbf{P}^{ij}$, in eqn (13), contain node displacements and tractions or interactive forces defined along the interface. Writing again eqn (13), now dividing the boundary value vectors into two parts, interface values, $\mathbf{U}^{ij}$ and $\mathbf{P}^{ij}$ and external values, $\mathbf{U}^{ie}$ and $\mathbf{P}^{ie}$, taking into account the equilibrium and displacement compatibility conditions, eqn (14), and joining them together the final system of algebraic equations for the combined body is,

$$\begin{bmatrix} H^{ie} & H^{ij} & -G^{ij} & 0 \\ 0 & H^{ji} & G^{ji} & H^{je} \end{bmatrix} \begin{Bmatrix} \mathbf{U}^{ie} \\ \mathbf{U}^{ij} \\ \mathbf{P}^{ji} \\ \mathbf{U}^{je} \end{Bmatrix} = \begin{bmatrix} G^{ie} & G^{ij} & 0 & 0 \\ 0 & 0 & G^{je} & G^{ji} \end{bmatrix} \begin{Bmatrix} \mathbf{P}^{ie} \\ \bar{\mathbf{P}}^{ij} \\ \mathbf{P}^{je} \\ \bar{\mathbf{P}}^{ji} \end{Bmatrix} + \begin{Bmatrix} \mathbf{A}^i \\ \mathbf{A}^j \end{Bmatrix} \tag{15}$$

where $\bar{\mathbf{P}}^{ij}$ represents prescribed surface forces along the contact.

As already mentioned before, expression (15) can be easily generalised for the multiple sub-region case.

For dynamic problems, it is important to take into account appropriate rearrangements of eqns (7) and (9) concerning three consecutive time steps for both finite and boundary element time integration schemes. It is also important to observe that compatibility is enforced only for node translations. Rotations have been left free, although their compatibility could be enforced as well if the proper integral representation for the boundary element formulation were considered. This alternative procedure is not an easy task due to singularities that may be found at non-smooth internal contact points. However, the numerical convergence of the solution obtained for many performed elastostatic and elastodynamic analyses indicates that the non-conforming scheme adopted here is a reliable coupling model. It is worth noting that for a single and straight pile the torsional rotation should be constrained.

5. Examples

Three examples have been selected to illustrate the formulation presented in this work. In these cases stiffened domains subjected to static and dynamic loads are analysed.

In the first example, the elastic half plane medium reinforced by a 0.61 m diameter circular cross section pile 6.1 m in length is subjected to sudden longitudinal, lateral and flexural loads, as can

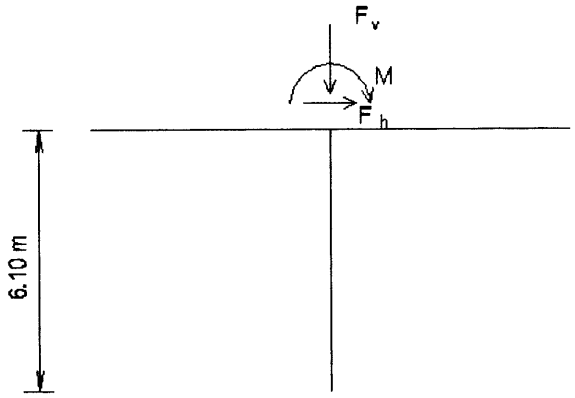

Fig. 3. Pile geometry and applied loads.

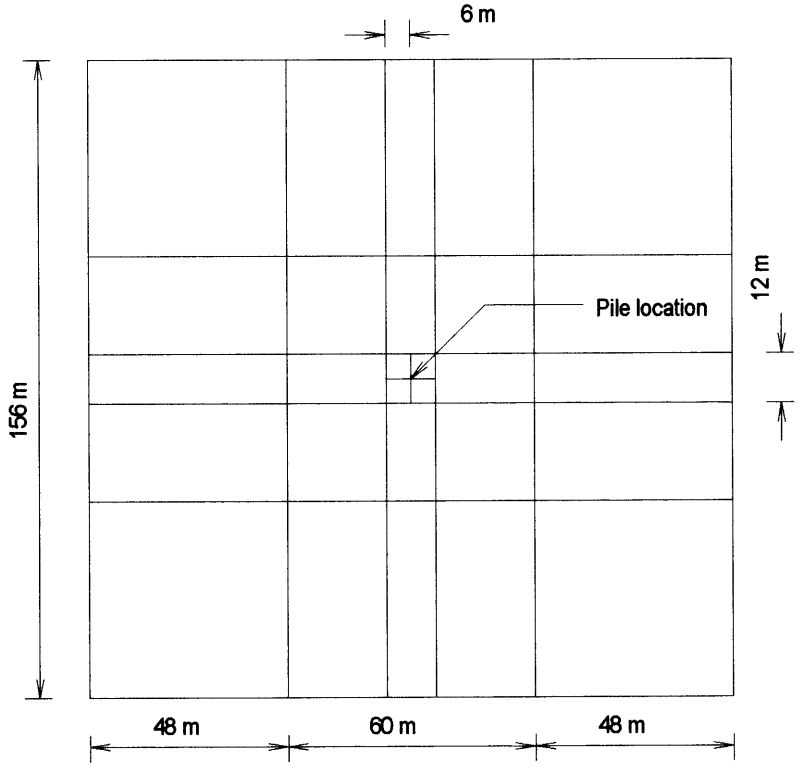

Fig. 4. Free surface discretization.

be seen in Fig. 3. Figure 4 presents the half space free surface discretization adopted to run this problem. In order to complete the discretization, ten finite beam elements are taken to describe the pile. The static results are compared with the numerical solution presented in Vallaban and

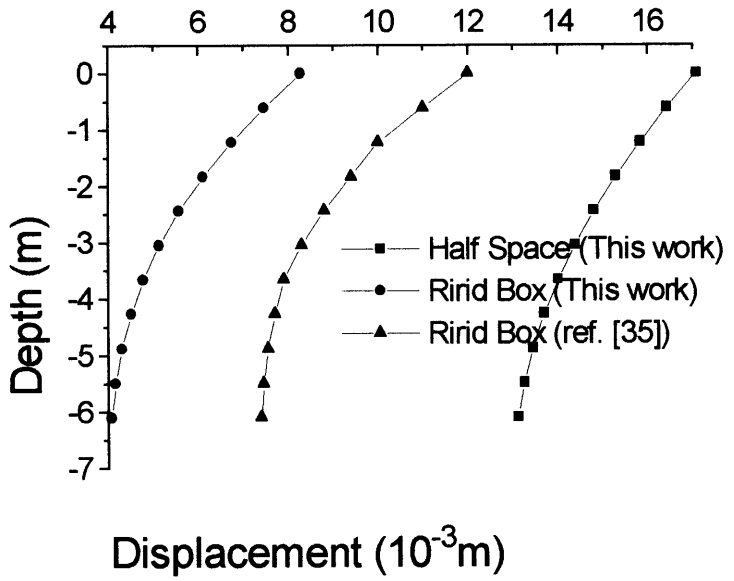

Fig. 5. Vertical load case: (a) vertical displacements; (b) interface forces.

Sivakumar (1986) where the pile is confined in a $6.1 \times 6.1 \times 12.2$ m^3 parallelepiped box region, for which horizontal displacements along the vertical sides are constrained, while null vertical displacements are enforced over the horizontal bottom plane. The same analysis has also been made, assuming the soil media as an infinite half space. Static and dynamic analyses have been carried out assuming the following material properties: $E_{\text{pile}} = 21{,}000{,}000$ N m^{-2}; $E_{\text{soil}} = 210{,}000$ N m^{-2}; $v_{\text{pile}} = 0.2$; $v_{\text{soil}} = 0.2$; $\rho_{\text{pile}} = 7000$ kg m^{-3} and $\rho_{\text{soil}} = 2000$ kg m^{-3}. For this dynamic analysis, some additional data have been assumed: $\Delta t = 0.2$ s and the pile viscous damping parameter $av = 0.4$.

After running the static case, all computed results together with the solution obtained by Vallaban and Sivakumar (1986) are displayed for comparison, in Figs 5–7. As can be seen, those solutions agree very well with the exception of one case. The main differences are probably due to the kind of boundary conditions assumed for each case. Having observed the good performance achieved for the static case, the analysis has been continued to verify how the formulation behaves when dealing with dynamic problems. For that case, the computed results are displayed in Figs 8–11. As can be seen, those numerical values obtained by using the proposed coupled formulation are very stable. Therefore, the transient BEM formulation achieved by using the particular fundamental solution due to distributed unit impulse gives stable results even when its algebraic relations are written for problems exhibiting a reasonable geometric complexity, in this case modified by coupling them with finite element relations.

In the second example, a short reinforced beam is analysed when submitted to a sudden tangential force. The beam is now treated as a three-dimensional domain, whereas the reinforcement bars are modelled by finite elements. In order to run this problem, the following material properties were assumed for the continuum media: $v = 0.30$; $E_c = 0.52 \times 10^8$ N m^{-2}, $\rho = 1.8 \times 10^{-3}$ kg m^{-3}. The time interval $\Delta t = 0.933 \times 10^{-2}$ s was taken to perform the integral along the time. The

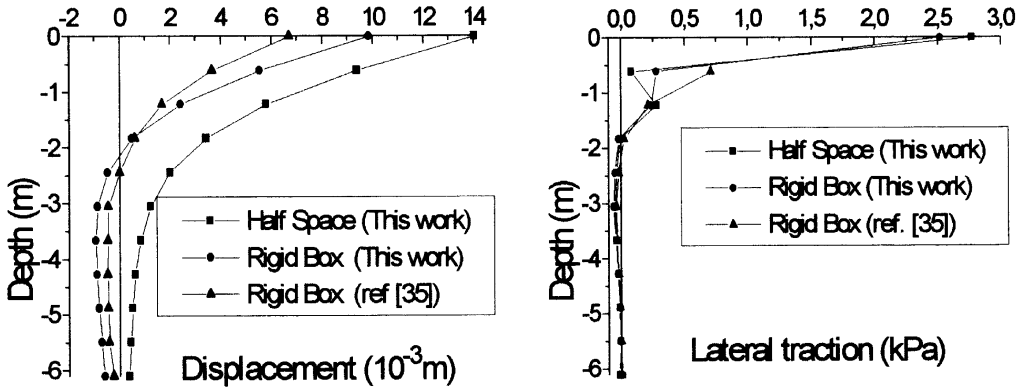

Fig. 6. Horizontal load case: (a) horizontal displacements; (b) interface forces.

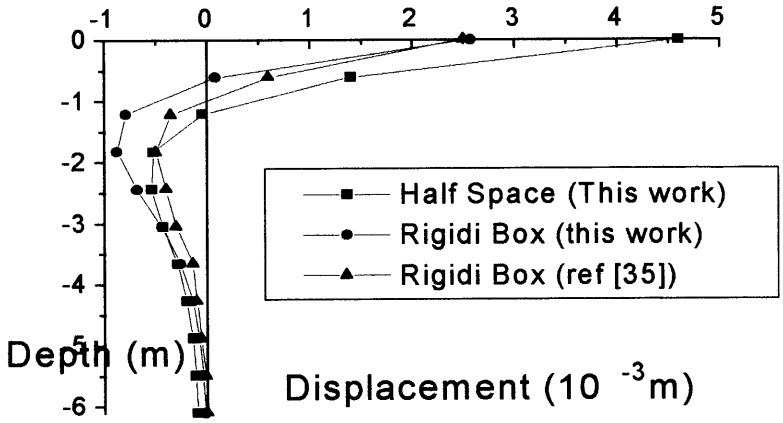

Fig. 7. Horizontal displacements for the applied moment.

tangential force applied over the beam end is assumed to be proportional to the Heaviside distribution along the time. In space, the applied load shows a parabolic shape defined by the maximum value, $p_0 = 1000$ N m^{-2}, at centre and zero at the edges of the loaded side, as shown in Fig. 12. No relaxed condition has been imposed to run this problem, therefore the expected results exhibit the complete bending behaviour due to both normal and shear deformations. The results computed by considering the non-reinforced beam are practically the same ones obtained by Araujo (1994), where the Dirac's Delta fundamental solution with linear time approximation and $\Delta t = 0.52 \times 10^{-2}$ s were adopted. Figure 13 shows the reinforced body cross section with two inside bars of 0.2 m diameter. For this case, Young modulus $E_b = 0.26 \times 10^9$ N m^{-2} has been assumed, while the same mass density was adopted.

Again, the accuracy or the formulation is observed (see Fig. 14), when comparing the dynamic responses for the non reinforced case. As in the first example, the results are very stable, showing

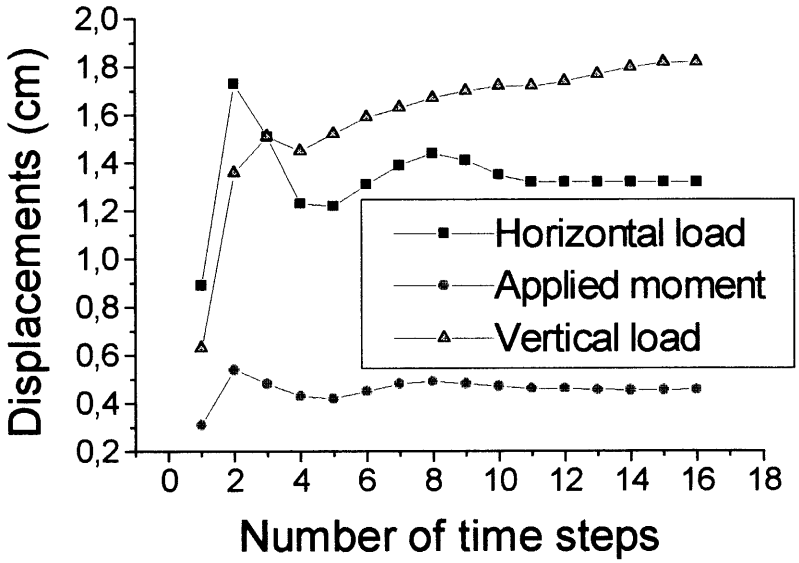

Fig. 8. Dynamic displacements at pile top end.

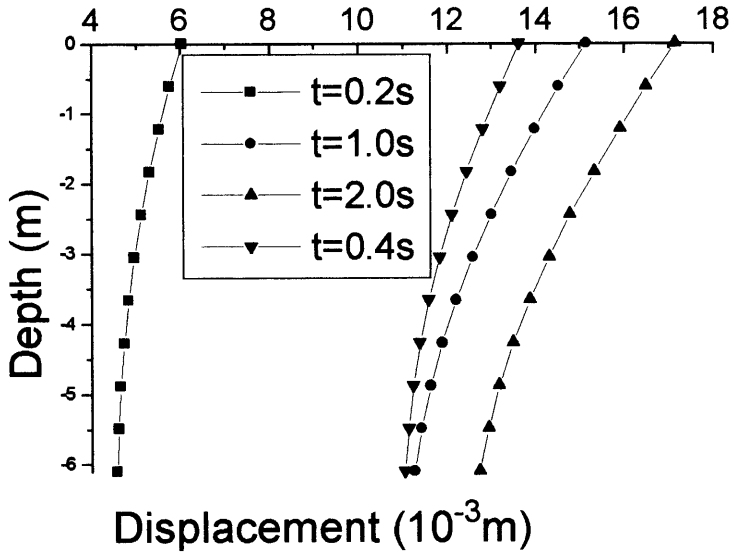

Fig. 9. Dynamic vertical displacements along the pile under vertical loads.

that the modification introduced by the finite element relations does not disturb the performance of the original BEM approach.

The last numerical example consists of analysing the movements of two towers connected to the 3D half space. One third of each tower is inserted into the 3D domain to guarantee a flexible connection. A suddenly applied concentrated load (4,000,000) is applied to the free end of one

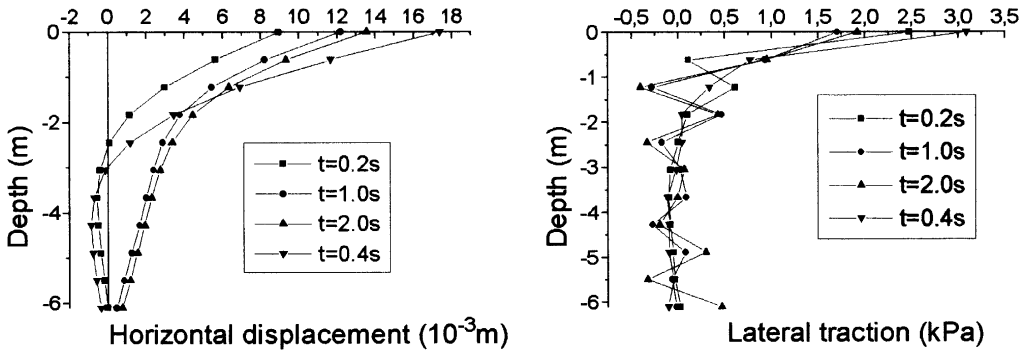

Fig. 10. Dynamic horizontal displacements and contact forces along the pile under horizontal loads.

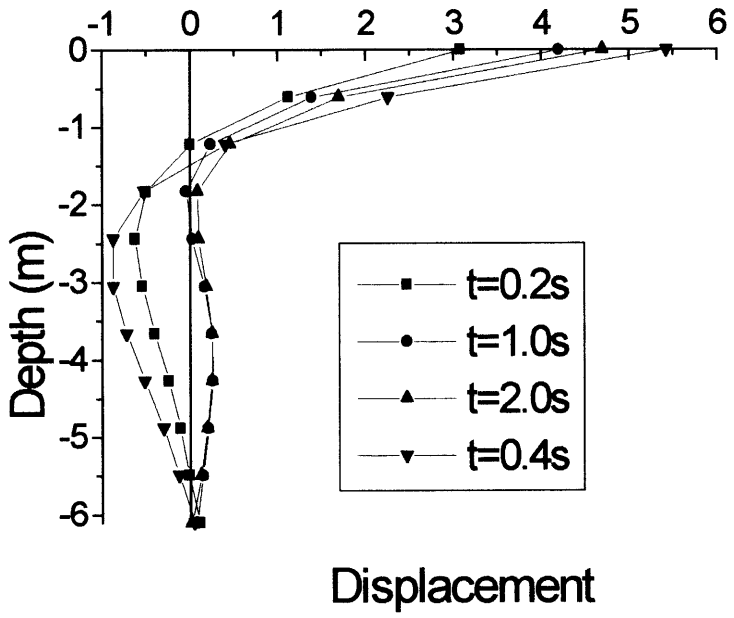

Fig. 11. Dynamic horizontal displacement along the pile due to the applied moment.

tower, as illustrated in Fig. 15a in which the geometry of the structural system is given. Fifteen cubic finite elements have been adopted to discretize each tower. The numerical solution has been obtained by assuming the following parameters for the towers and the 3D half space (units: dm, kg and s).

Towers: Young's modulus ($E = 2.1 \times 10^9$), mass density ($\rho = 6$), transversal section area ($A = 85.6$), inertia momentum (I = 1166.66).

Half space media: Young's modulus ($E = 2.6 \times 10^7$), mass density ($\rho = 2$) and Poisson's ratio ($v = 0.33$).

Time step: $\Delta t = 0.02264$ s.

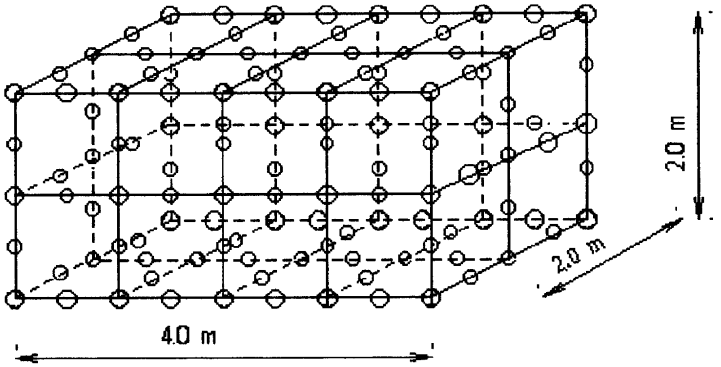

Fig. 12. Beam geometry and discretization.

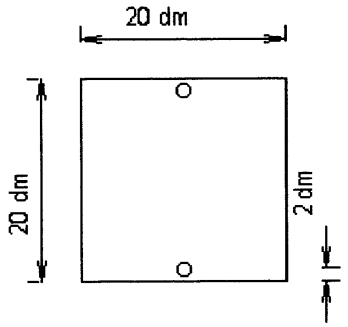

Fig. 13. Beam cross section with reinforcing bars.

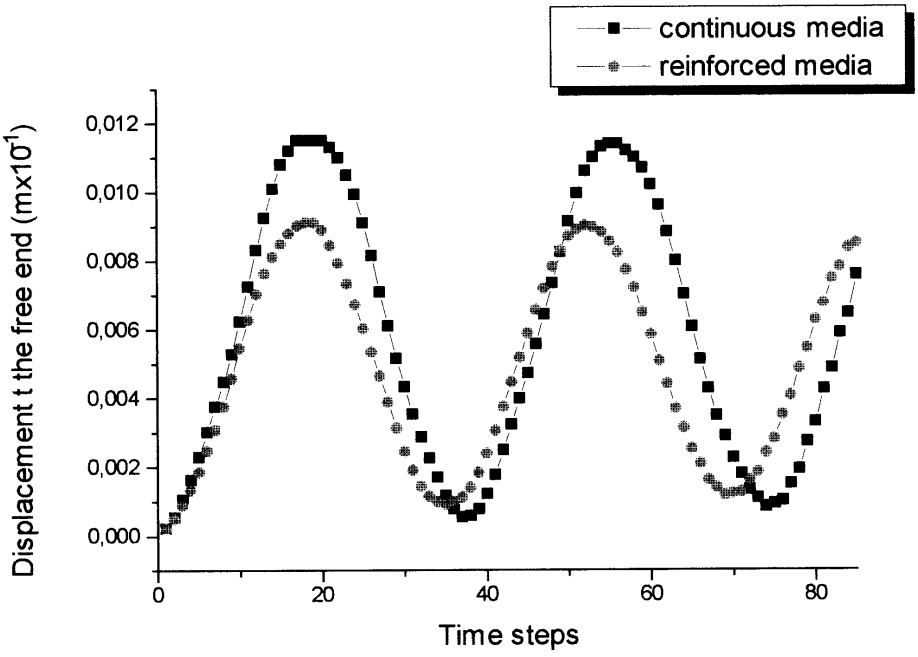

Fig. 14. Free end displacements for the reinforced and non reinforced cases.

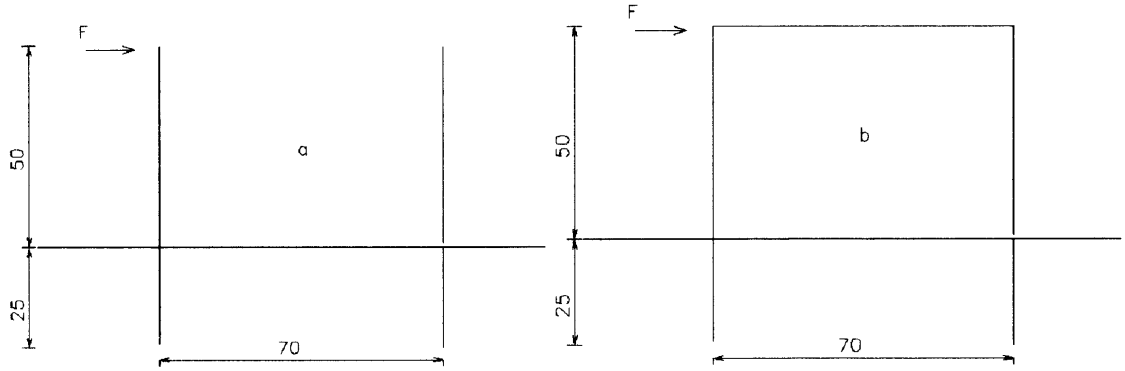

Fig. 15. Two fixed towers and a frame connected to the half space. Geometry and load: towers: Young's modulus ($E = 2.1 \times 10^9$), mass density ($\rho = 6$), transversal section area ($A = 85.6$), inertia momentum ($I = 1166.66$); half-space media: Young's modulus ($E = 2.6 \times 10^7$), mass density ($\rho = 2$) and Poisson's ratio ($v = 0.33$); time-step: $\Delta t = 0.02264$ s.

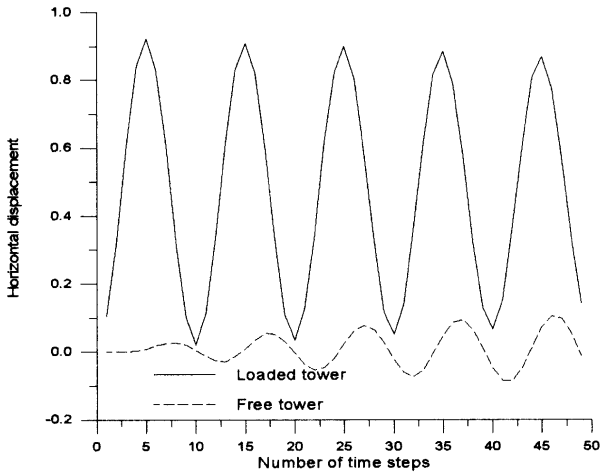

Fig. 16. Top of towers horizontal displacement.

The results obtained in terms of displacements, for the two independent towers, are displayed in Fig. 16. As can be seen, the loaded tower movements exhibit a little geometrical damping, while the free tower is excited by waves propagating through the soil.

This analysis is extended to analyse the behaviour of a two dimensional frame connected to the half space. The two tower ends are restrained by assuming between them a flexible horizontal beam, as illustrated in Fig. 15b. The displacement profile obtained for this situation is rather different than the previous case (see Fig. 17) pointing out the influence of the increased stiffness of the whole system. However, the time behaviour is quite similar, because the effects of the stiffness and mass variations compensate each other.

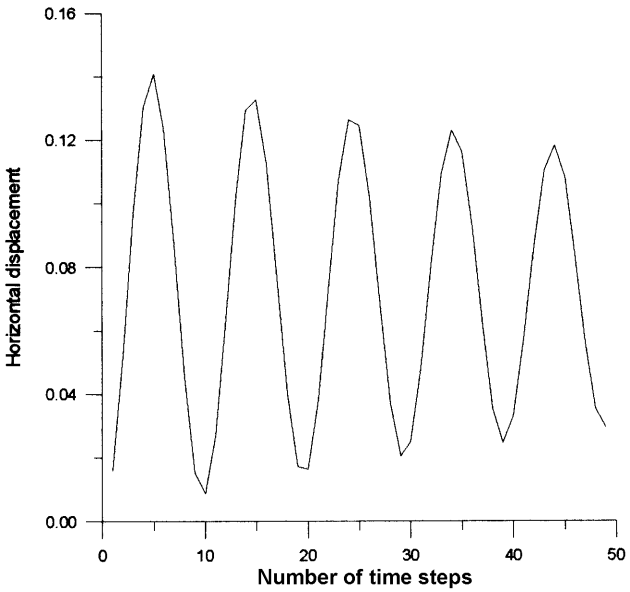

Fig. 17. Horizontal displacement at frame top.

6. Conclusions

The coupling of a finite element beam with a three-dimensional continuum body modelled by the boundary element method for both static and dynamic problems has been successfully implemented. The proposed technique is general and very useful for practical purposes such as soil-structure interaction and composite materials. The examples chosen in this article illustrate the high accuracy and stability achieved by this proposed numerical model. Although the technique is already suitable for practical application, improvements may be achieved. For instance, a more general hole element to precisely describe curved holes inside the continuum media can be easily implemented to improve the contact model. Physical non-linear behaviour over the contact between the continuum media and the beam element can eliminate undesirable stress concentrations as well. This will reduce the wave shape of the interface stresses improving the step by step procedure performance.

References

Antes, H., Steinfeld, B.A., 1992. Boundary Formulation Study of Massive Structures Static and Dynamic Behaviour. In: Brebbia, C.A. et al. (Eds.). Boundary Elements XIV 2, 27–42, Comp. Mech. Pub. & Elsevier Sc. Pub.

Araujo, F.C., 1994. Zeitberreichslösung linearer dreidimensionaler probleme der elastodynamik mit einer gekoppelten BE/FE—Methode. Ph.D. thesis, Technische Universität Brauschweig, Brauschweig, Germany.

Barreto, S.F.A., Coda, H.B., Venturini, W.S., 1996. Plate Soil Elastodynamic Coupling Using BEM. In: Brebbia, C.A. et al. (Eds.). Boundary Elements XVIII, CMP Pub., p. 363–372.

Bathe, K.J., 1982. Finite element procedures in engineering analysis. Englewood Cliffs, Prentice Hall.

Beer, G., Watson, J.O., 1992. Introduction to Finite and Boundary Element Methods for Engineers. John Wiley & Sons, New York.
Beskos, D.E., 1987. Boundary element methods in dynamic analysis. Appl. Mech. Rev. 40, 1–23.
Beskos, D.E., 1997. Boundary element methods in dynamic analysis: Part II (1986–1996). Appl. Mech. Rev. 50, 149–197.
Brebbia, C.A., Domingues, J., 1984. Boundary Elements: An introductory course. CMP Publications, Southampton
Brebbia, C.A., Telles, J.C.F., Wrobel, L.C., 1984. Boundary Element Techniques. Springer–Verlag, Berlin.
Clough, R.W., Penzien, J., 1975. Dynamics of structures. McGraw–Hill.
Coda, H.B., 1993. Three-dimensional transient analysis of structures by a BEM/FEM combination. Ph.D. thesis, University of São Paulo (Br), (in Portuguese).
Coda, H.B., Venturini, W.S., 1995a. Three-dimensional transient BEM analysis. Computer and Structures 56 (5), 751–768.
Coda, H.B., Venturini, W.S., 1995b. Three-dimensional elastodynamic formulation with domain initial conditions. In: Brebbia, C.A. et al. (Eds.). Boundary Elements XV. CML Pub., Southampton.
Coda, H.B., Venturini, W.S., 1995c. Numerical evaluation of flat singular boundary elements in elastostatics and elastodynamics. Boundary Elements Communications 6, 6–10.
Coda, H.B., Venturini, W.S., 1995d. Non-singular time-stepping BEM for transient elastodynamic analysis. Engineering Analysis with Boundary Elements 15, 11–18.
Coda, H.B., Venturini, W.S., 1996a. Further improvements on three dimensional transient BEM elastodynamics analysis. Engineering Analysis with Boundary Elements 17, 231–243.
Coda, H.B., Venturini, W.S., 1996b. A simple comparison between two 3D time domain elastodynamic boundary element formulations. Engineering Analysis with Boundary Elements 17, 33–44.
Coda, H.B., Venturini, W.S., 1996c. A Smooth Fundamental Solution for 3D Time Domain BEM. In: Brebbia, C.A. et al. (Eds.). Boundary Elements XVII. CM Pub., p. 259–267.
Coda, H.B., Venturini, W.S., 1996d. Time Domain BEM/FEM Approach Applied to Elastodynamic Analysis. In: Joint Conference of Italian Group of Computational Mechanics and CILAMCE. Proceedings. Università Degli Studi di Padova, p. 373–376.
Ferro, N.C.P., Venturini, W.S., 1992. BEM-FEM Coupling for Building Structure Analysis. In: Brebbia, C.A. et al. (Eds.). Boundary Elements XIV. CMP Publications, Southampton.
Guan, F., Novak, M., 1994. Transient response of a group of rigid strip foundations. Earthquake Engineering and Structural Dynamics, 23, 671–685.
Karabalis, D.L., Beskos, D.E., 1984. Dynamics response of 3-D rigid surface foundations by time domain boundary element method. Earthquake Engineering and Structural Dynamics 12, 73–93.
Kutt, H.R., 1975. WISK 178: quadrature formulae for finite-part integrals. Pretoria, National Research Institute for Mathematical Sciences. 156 p. (CSIR Special Report).
Lachat, J.C., Watson, J.O., 1976. Effective numerical treatment of boundary integral equations: a formulation for three-dimensional elastostatics. Int. J. Num. Methods Eng. 10, 991–1005.
Luco, J.E., Barros, C.P., 1994. Seismic response of a cylindrical shell embedded in a layered viscoelastic half-space Part I and II. Earthquake Engineering and Structural Dynamics 23, 553–567.
Mansur, W.J., 1988. Boundary element method applications in two-dimensional transient elastodynamics. In: Brebbia, C.A. (Ed.). Boundary elements X. Southampton, Springer–Verlag, Berlin 4, 387–399.
Stamos, A.A., Beskos, D.E., 1995. Dynamic analysis of large 3D underground structures by the BEM. Earthquake Engineering and Structural Dynamics 24, 917–934.
Stokes, G.G., 1849. On the dynamical theory of diffraction. Transactions of the Cambridge Philosophical Society 9, 1.
Vallabhan, C.V.G., Sivakumar, J., 1986. Coupling of BEM and FEM for 3D problems in geotechnical engineering. In: 2nd Boundary Element Technology Conference, MIT, Massachusetts, USA. Proceedings 675–686.
Warburton, G.B., 1976. The Dynamic behaviour of structures. 2nd ed. Pergamon Press, Oxford.
Zienkiewicz, O.C., 1980. El metodo de los elementos finitos. Barcelona, Revertè.